Computation of absorbing boundary conditions at the discrete level for acoustic waves in the frequency domain

Denis Duhamel

Computation of absorbing boundary conditions at the discrete level for acoustic waves in the frequency domain

Denis Duhamel

Ecole des Ponts ParisTech, Laboratoire Navier, IFSTTAR/CNRS/UPE
6 et 8 Avenue Blaise Pascal,
Cité Descartes, Champs sur Marne,
77455 Marne la Vallée, cedex 2, France
Tel: + 33 1 64 15 37 28
Fax: + 33 1 64 15 37 41
email : denis.duhamel@enpc.fr

Number of pages : 25

Number of figures : 9

Number of tables : 6

Preprint submitted to Elsevier *18 August 2019*

Abstract

The calculation of wave radiation in exterior domains by finite element methods can lead to large computations even if we consider linear problems in the frequency domain as in this article. Here, we study two-dimensional acoustics described by the Helmholtz equation. A large part of the exterior domain is meshed and this computational domain is truncated at some distance where local or global boundary conditions are imposed at this artificial boundary. These conditions at finite distance must simulate as closely as possible the exact radiation condition at infinity and are generally obtained by discretizing an operator on the boundary.

Here, we propose a different approach, still based on the finite element method. Instead of finding an absorbing operator and then discretizing it, we will estimate the absorbing operator directly at the discrete level and build a sparse matrix approximating the absorbing condition. This discrete absorbing matrix is added to the dynamic stiffness matrix of the problem which is then solved in a classical way. The coefficients of the absorbing matrix are found from the solutions of small size linear systems for each node on the radiating boundary. This is done using a set of radiating functions for which a boundary condition is written. The precision of the method is estimated from the number of functions in the test set and from the number of coefficients allowed in the sparse matrix. Finally, some examples are computed to validate the method.

Key words: Finite Element, absorbing boundary, acoustics, Helmholtz equation, frequency domain, exterior domain

1 Introduction

Solving the Helmholtz equation in unbounded domains is important in many problems of mechanics and physics, for instance for the acoustic radiation or diffraction around a body immersed in a fluid. Using the finite element method to solve this problem, one has to define a finite truncated domain whose solution should be as close as possible to the solution on the unbounded domain. For this, it is necessary to define a boundary condition at the exterior of this truncated domain. This condition at finite distance must simulate as closely as possible the exact radiation condition at infinity. This boundary condition could be global or local depending if all the degrees of freedom on the boundary are connected or if a given node is only coupled to a limited number of nodes around it.

Among the global approaches we find the Dirichlet to Neumann (DtN) condition proposed by [1,2], mainly for simple exterior geometries such as circles or spheres for which the solution in the exterior domain is solved analytically, or

the boundary element method described in many classical textbooks like [3–6]. These methods give accurate results but need full matrices and consequently lead to heavy computations. So they will not be considered in this article and we will concentrate on methods preserving the sparsity of the finite element formulation.

In local methods, on the contrary, the condition at a boundary node involves only a limited number of neighbouring nodes. They can be classified into mainly three sets: those involving only the degrees of freedom of the domain, those with additional degrees of freedom at nodes on the boundary and those with an additional domain. Concerning the absorption conditions which do not involve additional variables or domains, a first possibility is using infinite elements as proposed by [7–12]. These are elements extending at infinity and satisfying the Sommerfeld radiation condition. However, it needs the development of special elements based on functions with outwarding propagation wave-like behaviour in the radial direction and its efficiency is limited. Other absorbing boundary conditions involving differential operators of different orders on the boundary were proposed by different authors [13–16]. These relations were improved by Bayliss and Turkel [17,18] using sequences of local non-reflecting boundary conditions in spherical and cylindrical coordinates. Comparisons between infinite elements and these absorbing boundary conditions were also made by [19]. Finally [20,21] modified the conditions to get absorbing conditions for waves at some discrete angles from the normal. However, all these conditions are difficult to implement above the second order because of the high order derivatives involved in their formulations and can have difficulties at corners [22].

More efficient boundary conditions can be obtained by the addition of variables on the exterior surface as in [23,24] or more recently by [25]. A review of these methods is made by [26]. They involve only second order derivatives of the auxiliary variables and so can be efficiently implemented. However, they need additional degrees of freedom and a special treatment of the differential operators on the boundary.

Another possibility is the surrounding of the computational domain by absorbing layers as was first considered by [27,28]. This was improved by [29,30] who proposed the perfectly matched layer by surrounding the computational domain with a layer of elements in which the wave equation is analytically continued into complex coordinates. With a correct choice of the size of the layer and the parameters of the absorbing layer, very efficient absorptions of waves can be obtained. This however can add a non negligible number of degrees of freedom to the problem and the optimal parameters in the absorbing layer are not so easy to find. Several developments of the method and its optimisation can be found in [31,32]. Comparisons between high-order boundary conditions, perfectly matched layers and different absorbing conditions were

studied for instance by the review papers of [33–35].

Most of the precedent absorbing boundary conditions are written at the continuous level, but it can be interesting to write them at the discrete level. For instance, boundary conditions at the discrete level using the properties of periodic media were proposed by [36]. In [37] boundary conditions based on the PLM were written after discretisation of the equations and were found to be more efficient than their continuous versions. In [38] the authors proposed to build a discrete version of the DtN map. They obtained efficient results but the matrix giving the boundary condition is full in term of degrees of freedom on the boundary. Such a discrete approach is used in this paper in the aim of building an approximate absorbing boundary condition leading to a sparse matrix which can be efficiently integrated into the dynamic stiffness matrix of the problem. The following section presents the problem formulation and the building of the discrete absorbing matrix. Then some examples are presented before the conclusion.

2 Problem formulation

2.1 Helmholtz equation

We consider the two-dimensional acoustic equation in the frequency domain in the exterior Ω_e of a bounded domain Ω_i of boundary Γ_i, see Fig.1. The

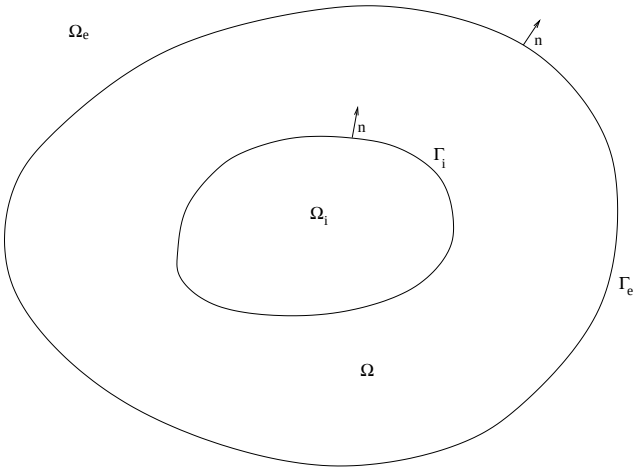

Fig. 1. Exterior domain.

Helmholtz equation with a Neumann boundary condition on Γ_i and a radiation condition at infinity is

$$\begin{aligned}
\Delta p + k^2 p &= f \quad on\ \Omega_e \\
\frac{\partial p}{\partial n} &= g \quad on\ \Gamma_i \\
\frac{\partial p}{\partial r} - ikp &= o(\frac{1}{\sqrt{r}})\ when\ r \to \infty
\end{aligned} \tag{1}$$

with f and g given functions representing the sources in the domain and at the boundary respectively. The domain Ω_e is truncated at some finite distance by the boundary Γ_e and the discrete problem is posed on the bounded domain Ω located between the surfaces Γ_e and Γ_i. Its variational formulation is

$$\int_\Omega (\Delta p + k^2 p) q dx = \int_\Omega f q dx \tag{2}$$

$$-\int_{\Gamma_i} \frac{\partial p}{\partial n} q ds + \int_{\Gamma_e} \frac{\partial p}{\partial n} q ds + \int_\Omega (-\nabla p.\nabla q + k^2 pq) dx = \int_\Omega f q dx \tag{3}$$

with q an arbitrary chosen test function and the exterior normals n at surfaces Γ_i and Γ_e. One assumes that the absorbing boundary condition can be written on the surface Γ_e as

$$\frac{\partial p}{\partial n} = \mathcal{A} p \tag{4}$$

where $\mathcal{A}$ is an operator acting on the pressure p inside Ω. So the variational formulation is now

$$\int_{\Gamma_e} (\mathcal{A} p) q ds + \int_\Omega (-\nabla p.\nabla q + k^2 pq) dx = \int_\Omega f q dx + \int_{\Gamma_i} g q ds \tag{5}$$

Unlike the usual absorbing boundary conditions, here the operator $\mathcal{A}$ is not limited to the boundary but involves points inside the domain Ω. One can expect a larger freedom to build a good absorbing operator. The purpose of this article is to build such an operator at the discrete level with limited computational costs and such that the matrix describing this operator at the discrete level is sparse.

2.2 Discretization of the absorbing operator

The absorbing operator is such that

$$\begin{aligned}
\int_{\Gamma_e} \frac{\partial p}{\partial n}(s) q(s) ds &= \int_{\Gamma_e} (\mathcal{A} p)(s) q(s) ds \\
&= \int_{\Gamma_e} \int_\Omega a(s,x) p(x) q(s) dx ds
\end{aligned} \tag{6}$$

where the operator $\mathcal{A}$ is defined by $(\mathcal{A} p)(s) = \int_{\Gamma_e} a(s,x) p(x) dx$. Denoting by $N_j^s(s)$ the shape functions on the boundary and $N_i^v(x)$ the shape functions on

the domain Ω, the discrete functions are such that

$$\begin{aligned} q(s) &= \sum_{j=1}^{j=n_s} q_j N_j^s(s) \\ \frac{\partial p}{\partial n}(s) &= \sum_{j=1}^{j=n_s} (\frac{\partial p}{\partial n})_j N_j^s(s) \\ a(s,x) &= \sum_{j=1}^{j=n_s} \sum_{i=1}^{i=n_v} A_{ji} N_j^s(s) N_i^v(x) \end{aligned} \tag{7}$$

with n_s the number of degrees of freedom on the boundary and n_v the number in the domain Ω. Thus we make the assumption that the kernel $a(s,x)$ can be approximated at the discrete level using the coefficients A_{ji} defining a matrix A. The purpose of the article is to find a good matrix A in the following such that the boundary condition (4) is absorbing. So relation (6) can be written as

$$\begin{aligned} \int_{\Gamma_e} \sum_{j=1}^{j=n_s} (\frac{\partial p}{\partial n})_j N_j^s(s) \sum_{l=1}^{l=n_s} q_l N_l^s(s) ds = \int_{\Gamma_e} \int_{\Omega} \sum_{j=1}^{j=n_s} \sum_{i=1}^{i=n_v} A_{ji} N_j^s(s) N_i^v(x) \\ \sum_{l=1}^{l=n_s} \sum_{m=1}^{m=n_v} p_m N_m^v(x) q_l N_l^s(s) dx ds \end{aligned} \tag{8}$$

leading to

$$\sum_{l=1}^{l=n_s} \sum_{j=1}^{j=n_s} M_{lj}^s q_l (\frac{\partial p}{\partial n})_j = \sum_{l=1}^{l=n_s} \sum_{j=1}^{j=n_s} \sum_{i=1}^{i=n_v} \sum_{m=1}^{m=n_v} M_{lj}^s A_{ji} M_{im}^v p_m q_l \tag{9}$$

with

$$\begin{aligned} M_{lj}^s &= \int_{\Gamma_e} N_l^s(s) N_j^s(s) ds \\ M_{im}^v &= \int_{\Omega} N_i^v(x) N_m^v(x) dx \end{aligned} \tag{10}$$

As relation (9) is true for an arbitrary q_l, one gets

$$\sum_{j=1}^{j=n_s} M_{lj}^s (\frac{\partial p}{\partial n})_j = \sum_{j=1}^{j=n_s} \sum_{i=1}^{i=n_v} \sum_{m=1}^{m=n_v} M_{lj}^s A_{ji} M_{im}^v p_m \tag{11}$$

so that in matrix form, one has

$$\mathbf{M}^s \mathbf{d} = \mathbf{M}^s \mathbf{A} \mathbf{M}^v \mathbf{p} \tag{12}$$

with $\mathbf{d}$ the vector of the normal derivatives of the pressure at the nodes of Γ_e, $\mathbf{p}$ the vector of the pressures at nodes in Ω and $\mathbf{A}$ the matrix made of the A_{ji} coefficients. From relation (12), one can remove the invertible mass matrix $\mathbf{M}^s$ and finally the vectors $\mathbf{p}$ and $\mathbf{d}$ are linked by

$$\mathbf{d} = \mathbf{A}\mathbf{M}^v\mathbf{p} \tag{13}$$

and one has to identify the absorbing matrix $\tilde{\mathbf{A}} = \mathbf{A}\mathbf{M}^v$.

2.3 Determination of the absorbing matrix

The solution of the problem can be expanded as

$$p(r,\theta) = \sum_{-\infty}^{+\infty} a_n H_n(kr) e^{in\theta} \tag{14}$$

The completeness of this expansion on the boundary was proved by [39–41]. One now has to find an approximation of the matrix $\tilde{\mathbf{A}} = \mathbf{A}\mathbf{M}^v$. One looks for a discrete operator acting on the pressure at nodes inside Ω such that the matrix $\tilde{\mathbf{A}}$ is sparse and the relation (13) is satisfied for outgoing waves such as those involved in the expansion (14).

For a node i at point $\mathbf{x}_i$ on the boundary, one considers N_i nodes i_j at points $\mathbf{x}_{i_j}$ in Ω with $j = 1...N_i$ in the neighbourhood of $\mathbf{x}_i$ and such that $\mathbf{x}_{i_1} = \mathbf{x}_i$. So the line i of the matrix $\tilde{\mathbf{A}}$ will have non zero coefficients only at nodes i_j. To find these coefficients, one writes equation (13) for Hankel functions of different orders n. Choosing a point $\mathbf{o}$ interior to Ω_i as the origin for the expansion (14), one should have

$$\frac{\partial}{\partial n_i}(H_n(k|\mathbf{x}_i - \mathbf{o}|)e^{in\theta_i}) = \sum_{j=1...N_i} a_j^i (H_n(k|\mathbf{x}_{i_j} - \mathbf{o}|)e^{in\theta_{i_j}}) \tag{15}$$

for $-N \leq n \leq N$, n_i the exterior normal at node i, a_j^i the coefficients of the matrix $\tilde{\mathbf{A}}$ to be found and θ_{i_j} the angular coordinate of $\mathbf{x}_{i_j}$ in polar coordinates. We define the vectors

$$\mathbf{f}_i = \begin{bmatrix} \frac{\partial}{\partial n_i}(H_{-N}(k|\mathbf{x}_i - \mathbf{o}|)e^{-iN\theta_i}) \\ ... \\ \frac{\partial}{\partial n_i}(H_0(k|\mathbf{x}_i - \mathbf{o}|)) \\ ... \\ \frac{\partial}{\partial n_i}(H_N(k|\mathbf{x}_i - \mathbf{o}|)e^{iN\theta_i}) \end{bmatrix} \quad , \quad \mathbf{a}_i = \begin{bmatrix} a^i_{i_1} \\ ... \\ a^i_{i_{N_i}} \end{bmatrix} \tag{16}$$

and the matrix

$$\mathbf{H}_i = \begin{bmatrix} H_{-N}(k|\mathbf{x}_{i_1} - \mathbf{o}|)e^{-iN\theta_{i_1}} & ... & H_{-N}(k|\mathbf{x}_{i_{N_i}} - \mathbf{o}|)e^{-iN\theta_{i_{N_i}}} \\ ... & & ... \\ H_0(k|\mathbf{x}_{i_1} - \mathbf{o}|) & ... & H_0(k|\mathbf{x}_{i_{N_i}} - \mathbf{o}|) \\ ... & & ... \\ H_N(k|\mathbf{x}_{i_1} - \mathbf{o}|)e^{iN\theta_{i_1}} & ... & H_N(k|\mathbf{x}_{i_{N_i}} - \mathbf{o}|)e^{iN\theta_{i_{N_i}}} \end{bmatrix} \tag{17}$$

Relation (15) can be put under the form

$$\mathbf{f}_i = \mathbf{H}_i \mathbf{a}_i \tag{18}$$

Its approximate solution is given by

$$\mathbf{a}_i = (\mathbf{H}_i^* \mathbf{H}_i)^{-1} \mathbf{H}_i^* \mathbf{f}_i \tag{19}$$

with * denoting the hermitian transpose of a matrix. The vector $\mathbf{a}_i$ gives the *ith* line of the matrix $\tilde{\mathbf{A}}$. As the matrix to be inverted can be ill conditioned the following regularisation is done

$$\mathbf{a}_i = (\mathbf{H}_i^* \mathbf{H}_i + \epsilon \mathbf{I})^{-1} \mathbf{H}_i^* \mathbf{f}_i \tag{20}$$

with ϵ a small parameter and $\mathbf{I}$ the identity matrix. Considering these relations for all nodes at the boundary, one gets the sparse matrix $\tilde{\mathbf{A}}$ describing an approximate absorbing boundary condition on Γ_e. More precisely, the computation of $\mathbf{M}^s \tilde{\mathbf{A}}$ is done element by element by decomposing as

$$\int_{\Gamma_e} (\mathcal{A}p)(s) q(s) ds = \sum_m \int_{\Gamma_e^m} (\mathcal{A}p)(s) q(s) ds \tag{21}$$

and the matrix $\tilde{\mathbf{A}}$ is computed on each element Γ_e^m at Gauss points and is added to the global matrix by discrete integration.

The discretisation of the other parts of the variation formulation (5) leads to the final discrete equation.

$$(\mathbf{K} - \mathbf{M}^s \tilde{\mathbf{A}} - k^2 \mathbf{M})\mathbf{p} = \mathbf{F} \tag{22}$$

which can be solved by classical solvers. $\mathbf{F}$ is the load vector resulting from the discretization of the right-hand side of relation (5). $\mathbf{M}$ is the mass matrix while $\mathbf{K}$ is the stiffness matrix.

If we compare for instance to infinite elements, they involve only nodes on the boundary. Here some nodes inside the domain are involved in the computation of the absorbing matrix. We can expect a better accuracy.

3 Numerical examples

3.1 Test problem

As a first example we consider an annular domain limited by an interior circle of radius $0.15m$ and an exterior circle of radius $0.3m$, see Fig.2(a) for the geometry and Fig.2(b) for the mesh. The sound velocity is $c = 340m/s$. The mesh is made of 11138 linear triangular elements with a total of 5765 nodes. This leads to ten nodes by wavelength up to the frequency $3500Hz$. A boundary condition is defined at the interior circle as the normal derivative of the sound pressure generated by a point source located at point $\mathbf{x}_s = (0.1m, 0)$ and is given by

$$g(\mathbf{x}) = -\frac{ik}{4}\frac{\mathbf{n}.(\mathbf{x}-\mathbf{x_s})}{|\mathbf{x}-\mathbf{x_s}|}H_1(k|\mathbf{x}-\mathbf{x_s}|) \tag{23}$$

with $\mathbf{x}$ the position of a node on the interior boundary Γ_i, $\mathbf{x_s}$ the position of the point source and n the normal at the boundary. The analytical solution is given by

$$p^{ana}(\mathbf{x}) = \frac{i}{4}H_0(k|\mathbf{x}-\mathbf{x_s}|) \tag{24}$$

and will be compared to various numerical solutions.

We define the errors e_g on the whole domain Ω and e_b on the exterior boundary Γ_e by

$$\begin{aligned} e_g^2 &= \frac{\sum_{i\ node\ in\ \Omega} |p_i^{num} - p_i^{ana}|^2}{\sum_{i\ node\ in\ \Omega} |p_i^{ana}|^2} \\ e_b^2 &= \frac{\sum_{i\ node\ in\ \Gamma_e} |p_i^{num} - p_i^{ana}|^2}{\sum_{i\ node\ in\ \Gamma_e} |p_i^{ana}|^2} \end{aligned} \tag{25}$$

with the superscripts *ana* and *num* denoting respectively the analytical and numerical solutions.

3.2 Selection of points to build the matrix $\tilde{\mathbf{A}}$

Different possibilities exist for choosing the N_i points to build the i^{th} line of matrix $\tilde{\mathbf{A}}$. For instance, one can choose the N_i closest nodes to the boundary node associated to line i. One can also take these points at random inside the domain Ω or take a mix of the two precedent possibilities taking for instance

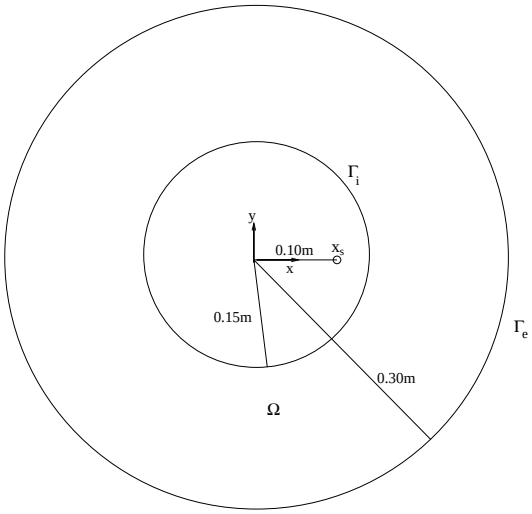

(a)

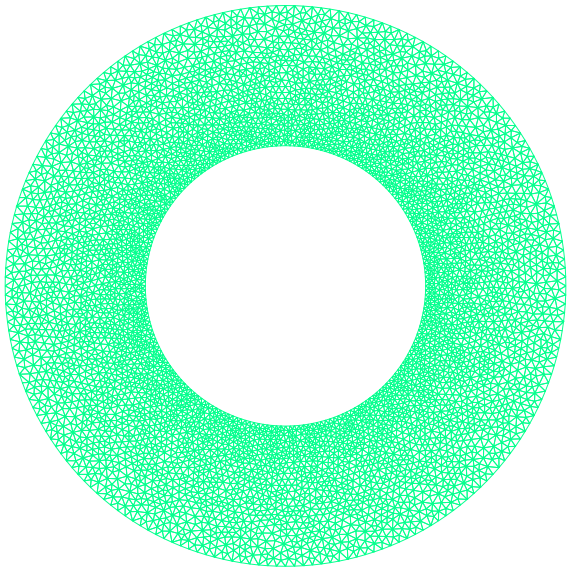

(b)

Fig. 2. (a) Annular domain and (b) its mesh.

$N_i/2$ points close to the boundary node and $N_i/2$ points at random. The errors associated to these possibilities are given in table 1 for the frequency $100Hz$ and the value $N_i = 20$. So for $N \leq 1$ we choose the strategy of taking the N_i nodes closest to the boundary node while for $N \geq 2$ we adopt the mix strategy. Fig.3 presents the nodes associated to a reference node on the boundary for these three possible choices.

Value of N	close to node	at random	mix of close and random
N=0	0.078	0.304	0.149
N=1	0.005	0.029	0.018
N=2	0.042	0.007	0.003
N=3	0.357	0.002	0.001
N=4	0.360	0.0007	0.0007

Table 1
Boundary error e_b for $N_i = 20$ points for different strategies for choosing the nodes in $\tilde{\mathbf{A}}$

3.3 Influence of different parameters

In Fig.4 four solutions in term of modulus of the pressure are plotted for different truncation orders N. The first three solutions are obtained by the present method with respectively $N = 0$, $N = 1$, $N = 2$ and the last one is the analytical solution for the frequency $100Hz$. These solutions are obtained by taking $N_i = 20$ coefficients for each boundary node in the building of the matrix $\tilde{\mathbf{A}}$. It can be seen that these solutions are a good approximation of the analytical solution even for the crudest solution with $N = 0$.

The numerical errors on the boundary and in the domain are given in table 2 for N between 0 and 4. Increasing N leads to a lower error as can be expected. The boundary error is a little larger than the domain error. One can see that the value $N = 1$ leads to good results. This value will be taken in the following unless otherwise specified.

Value of N	global error	boundary error
N=0	0.0585	0.0780
N=1	0.0033	0.0054
N=2	0.0017	0.0037
N=3	0.0005	0.0009
N=4	0.0003	0.0005

Table 2
Domain and boundary errors for different values of N at 100Hz

In Fig.5 the solution is plotted versus the number of points N_i used to build $\tilde{\mathbf{A}}$ with $N = 1$. Using $N_i = 2$ is clearly not enough. However, one can see that $N_i = 5$ gives a rather good solution which is still improved by using more points. Numerical values associated to the figure 5 are given in table 3. As excepted the error is decreasing when N_i increases as more nodes can be

involved in definition of the absorbing operator which becomes more accurate. One see that the error at the boundary is a little larger than the error on the whole domain. For a given value of N these errors should be limited and would still decrease if N is increased.

Number of nodes	global error	boundary error
$N_i = 2$	0.459	0.522
$N_i = 5$	0.010	0.013
$N_i = 10$	0.005	0.006
$N_i = 20$	0.003	0.005

Table 3
Error for different numbers of nodes used to build the matrix $\tilde{\mathbf{A}}$

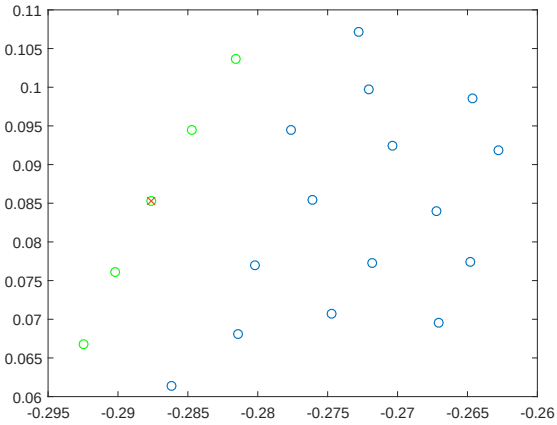

(a)

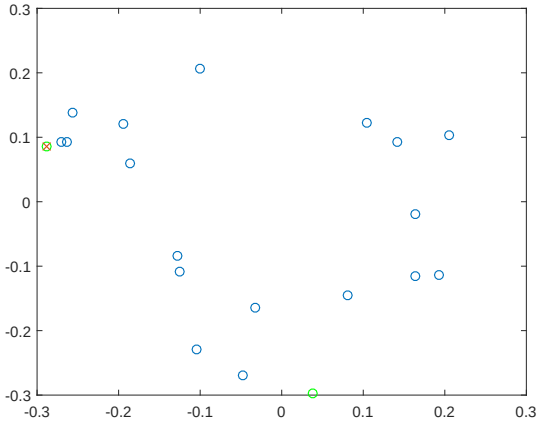

(b)

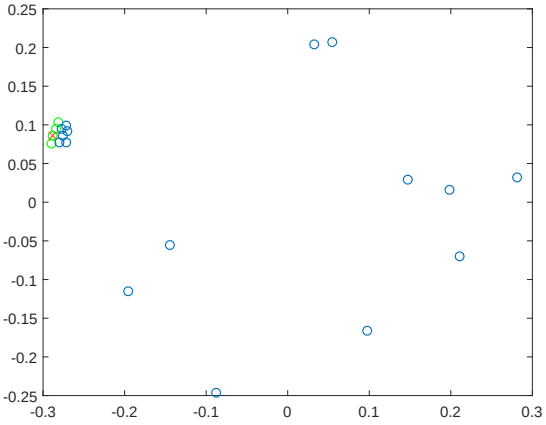

(c)

Fig. 3. Nodes associated to a reference node for the three possible strategies: (a) Closest nodes, (b) random nodes and (c) mixed strategy. The reference node on the boundary is noted by x, the nodes on the boundary are green and the nodes inside the domains are black.

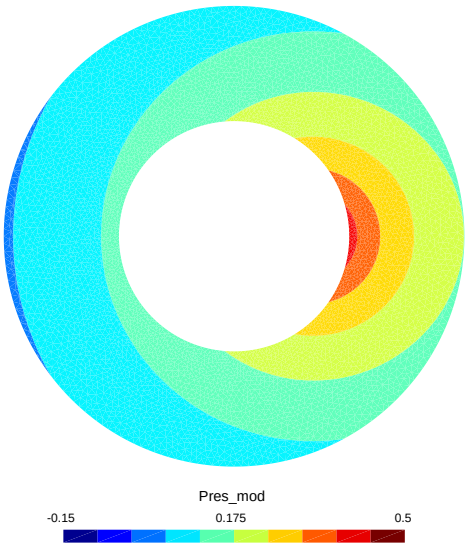

(a) $N = 0$

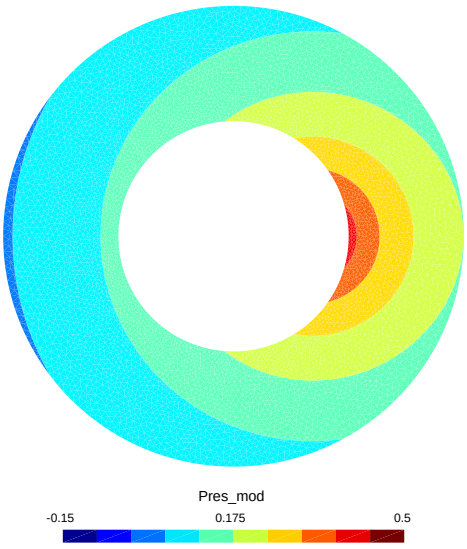

(b) $N = 1$

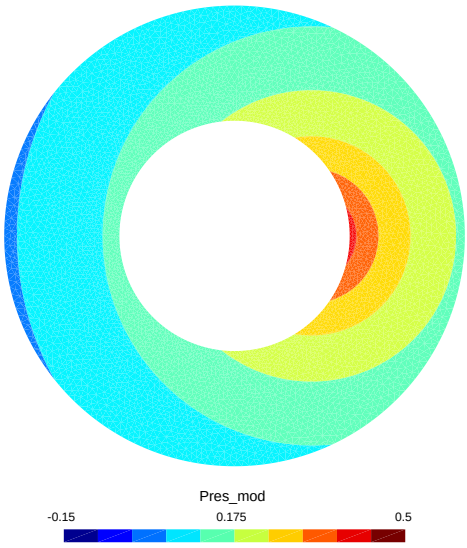

(c) $N = 2$

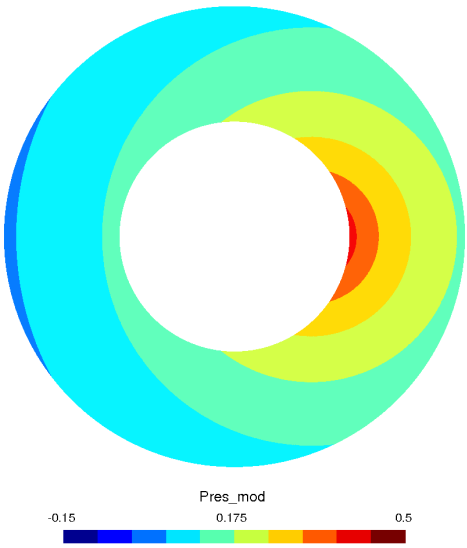

(d) Analytical solution at 100Hz

Fig. 4. Comparison of solutions at 100Hz for different N

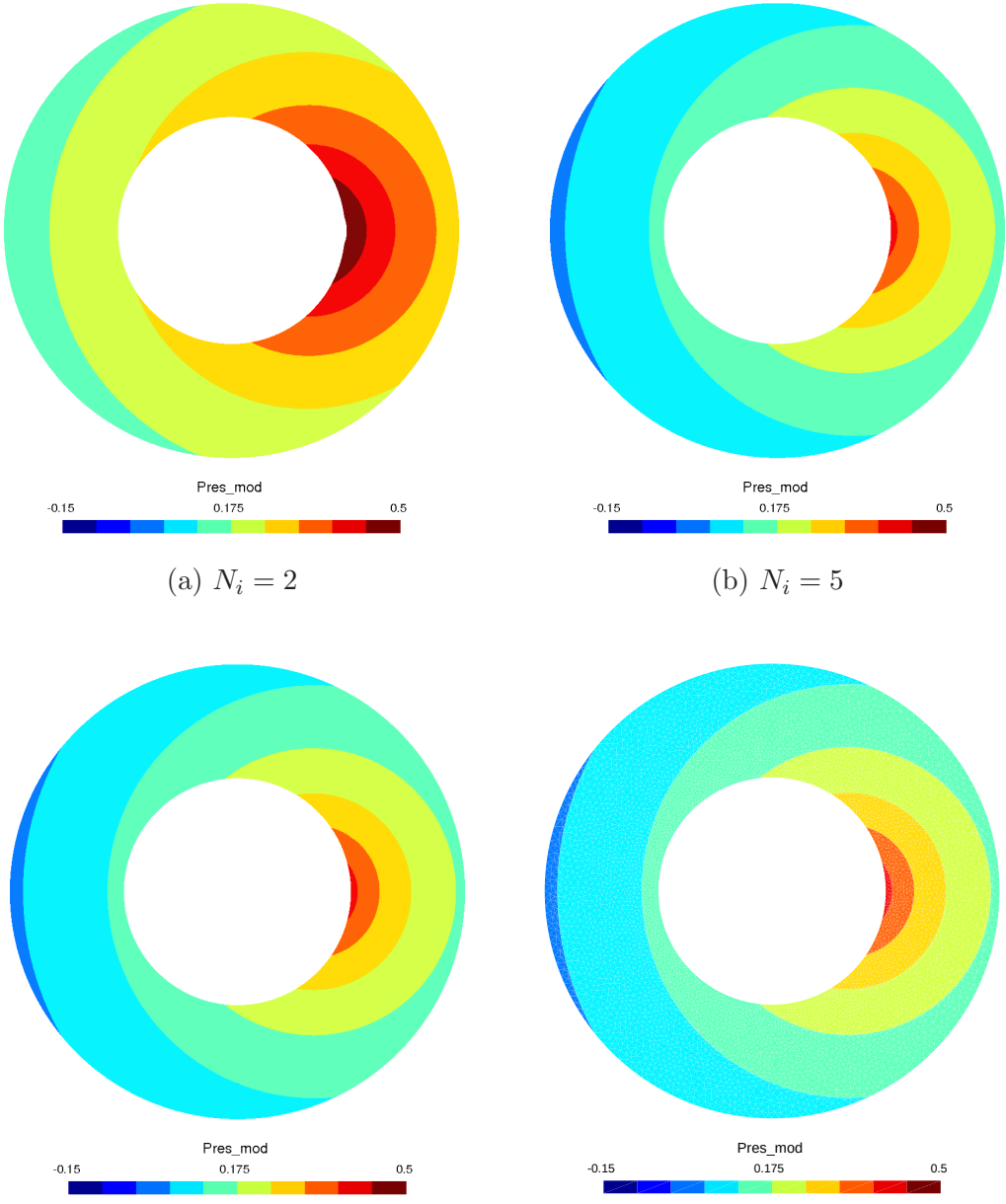

(a) $N_i = 2$ (b) $N_i = 5$

(c) $N_i = 10$ (d) $N_i = 20$

Fig. 5. Solutions for different numbers N_i of nodes used to define the matrix $\tilde{\mathbf{A}}$

Finally Fig.6 compares the analytical solutions and the numerical ones for different frequencies. Only $N_i = 2$ points are used which leads to crude estimates. While the solution at $100Hz$ shows important errors, the results at $300Hz$ and $1000Hz$ are much better. This shows that the condition for a limited number N_i of nodes is more efficient as the frequency increases as for other usual absorbing boundary conditions.

3.4 Comparison with other absorbing conditions

We will compare the solution of the present method to the computations obtained by the use of the following local and global boundary conditions

- Sommerfeld (S)
  $\frac{\partial p}{\partial n} = ikp$
- First order Bayliss and Turkel (FBT) (see [17])
  $\frac{\partial p}{\partial n} = (ik - \frac{1}{2R})p$
- Second order Bayliss and Turkel (SBT) (see [17,42])
  $\frac{\partial p}{\partial n} = -\frac{1}{2(ik-\frac{1}{R})}(2k^2 + \frac{3ik}{R} - \frac{5}{4R^2} + \frac{1}{R^2}\frac{\partial^2}{\partial\theta^2})p$
- Second order Feng (SF) (see [43])
  $\frac{\partial p}{\partial n} = (ik - \frac{1}{2R} + \frac{i}{8kR^2} + \frac{i}{2kR^2}\frac{\partial^2}{\partial\theta^2})p$
- DtN boundary condition on a circle given by (see [1])
  $$\frac{\partial p}{\partial n} = -{\sum_{n=0}^{\infty}}' \int_0^{2\pi} m_n(\theta - \theta')p(R,\theta')d\theta'$$
  $$m_n(\theta - \theta') = -\frac{k}{\pi}\frac{H_n^{(1)'}(kR)}{H_n^{(1)}(kR)}\cos n(\theta - \theta')$$

where the prime close to the sum means that a factor $\frac{1}{2}$ multiplies the term with $n = 0$. This condition should be very accurate and will provide a reference solution. For the following examples 11 terms are kept in the sum which was found to be sufficient for the frequency $2000Hz$. However the computing time is much longer than for the other boundary conditions.

The boundary condition with the present method is obtained for $N_i = 20$ and $N = 1$. Table 4 presents the errors in the domain for these different boundary conditions. It can be seen that the Sommerfeld condition is inaccurate except for high frequencies as it would be expected. The present method is denoted DLAC (Discrete Level Absorbing Condition). For DLAC1 the parameters are $N = 1$ and $N_i = 20$. For DLAC2, one has $N = 4$ and $N_i = 100$. The error

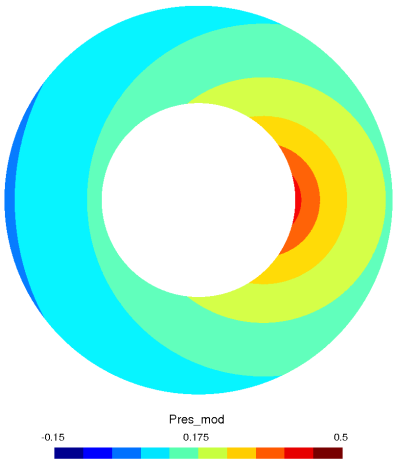

(a) Analytical solution 100Hz

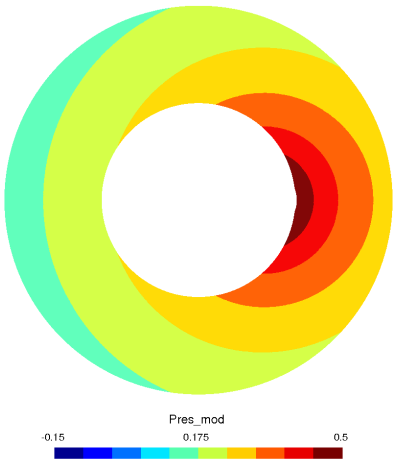

(b) Numerical solution 100 Hz

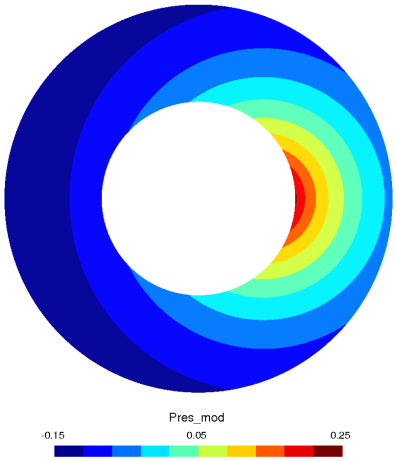

(c) Analytical solution 300Hz

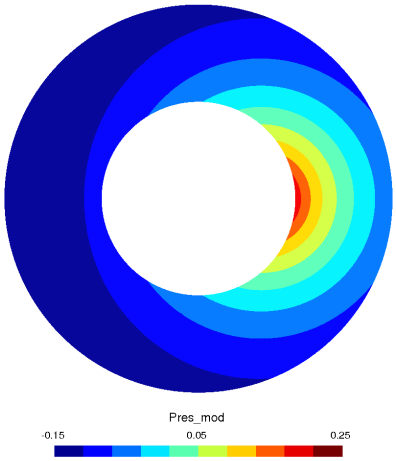

(d) Numerical solution 300 Hz

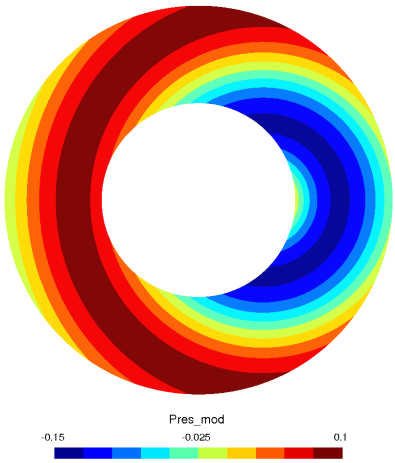

(e) Analytical solution 1000Hz

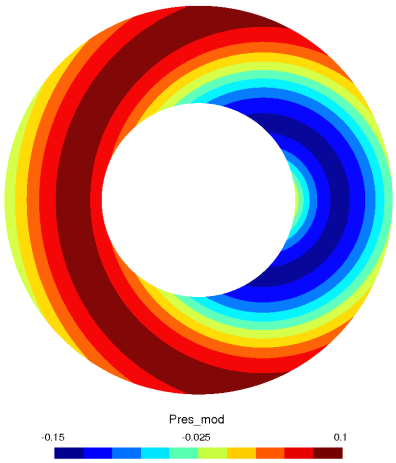

(f) Numerical solution 1000 Hz

Fig. 6. Solutions for different frequencies

Frequency	S	FBT	SBT	SF	DtN	DLAC1	DLAC2
10 Hz	4.527	0.455	0.542	0.845	$7.56\ 10^{-5}$	0.003	$1.37\ 10^{-4}$
50 Hz	1.200	0.266	0.386	0.390	$8.35\ 10^{-5}$	0.003	$1.40\ 10^{-4}$
100 Hz	0.665	0.162	0.286	0.176	$9.66\ 10^{-5}$	0.003	$1.45\ 10^{-4}$
500 Hz	0.160	0.041	0.028	0.018	$3.59\ 10^{-4}$	0.004	$4.59\ 10^{-4}$
1000 Hz	0.086	0.036	0.006	0.008	$1.14\ 10^{-3}$	0.003	$1.59\ 10^{-3}$
2000 Hz	0.050	0.033	0.006	0.007	0.006	0.007	0.022

Table 4
Error e_g in the domain for different boundary conditions

with DLAC1 method is stable over the whole frequency range and is especially much better than the other local boundary conditions for low and medium frequencies. The condition is not as accurate as the DtN condition but it is much faster. For $2000Hz$ the density of the mesh is the principal factor limiting the accuracy of the solution. For DLAC2, one recovers a precision close to the DtN with still a much faster solution except for high frequencies for which a simpler condition is better to avoid conditionning problems. This is described in relation (20). The matrix to be inverted suffers some conditioning problems. Another balancing of the matrix allows to reduce the error to $1.5\ 10^{-3}$. The optimal balancing of the matrix according to the number of points and the frequency needs further study.

3.5 Sparsity of matrices

Without absorbing boundary conditions one has to solve a problem with the matrix $\mathbf{K}$ while with absorbing boundary conditions the problem is solved with the matrix $\mathbf{K} - \mathbf{M}^v\tilde{\mathbf{A}}$. In table 5, we compare the number of non zero elements in the matrix $\mathbf{M}^v\tilde{\mathbf{A}}$ for different values of N_i and for the frequency $100Hz$. The case $N_i = 0$ means that we consider the matrix $\mathbf{K}$ only.

We see that even for the case $N_i = 20$ the increase in the number of non zeros element is limited to 10% and is only 1.9% for $N_i = 5$. If we consider the half bandwidth the increase is more noticeable. Fig.7 presents the sparsity patterns for matrices $\mathbf{K}$ and $\mathbf{K} - \mathbf{M}^v\tilde{\mathbf{A}}$ for the case $N_i = 10$. The reverse Cuthill-McKee ordering has been applied to make the matrices closer to the matrix used in the matlab solver. One can see that matrix $\mathbf{M}^v\tilde{\mathbf{A}}$ adds only a limited numbers of non zero elements.

Number of nodes	nnz($\mathbf{K} - \mathbf{M}^{\mathbf{v}}\tilde{\mathbf{A}}$)	% of non zeros coefficients	Average half bandwidth
$N_i = 0$	39571	0.12%	1.6%
$N_i = 2$	39586	0.12%	1.6%
$N_i = 5$	40327	0.12%	1.9%
$N_i = 10$	41401	0.12%	2.0%
$N_i = 20$	43886	0.13%	2.9%

Table 5
Number of non zeros elements in the matrix $\mathbf{K} - \mathbf{M}^v\tilde{\mathbf{A}}$ for different N_i

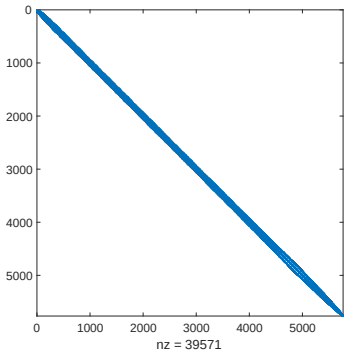

(a) Matrix $\mathbf{K}$

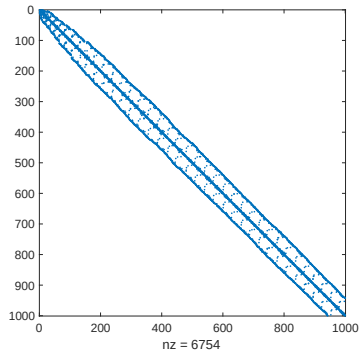

(b) Zoom on matrix $\mathbf{K}$

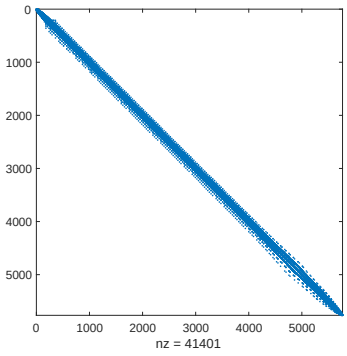

(c) Matrix $\mathbf{K} - \mathbf{M}^v\tilde{\mathbf{A}}$

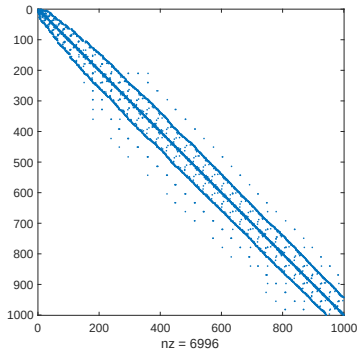

(d) Zoom on matrix $\mathbf{K} - \mathbf{M}^v\tilde{\mathbf{A}}$

Fig. 7. Non zeros elements for the matrices $\mathbf{K}$ and $\mathbf{K} - \mathbf{M}^v\tilde{\mathbf{A}}$

3.6 Case of domains with corners

We consider now the case of a square of size $0.6m \times 0.6m$ centred on the origin as an example of a domain with corners, see Fig.8(a). The square is

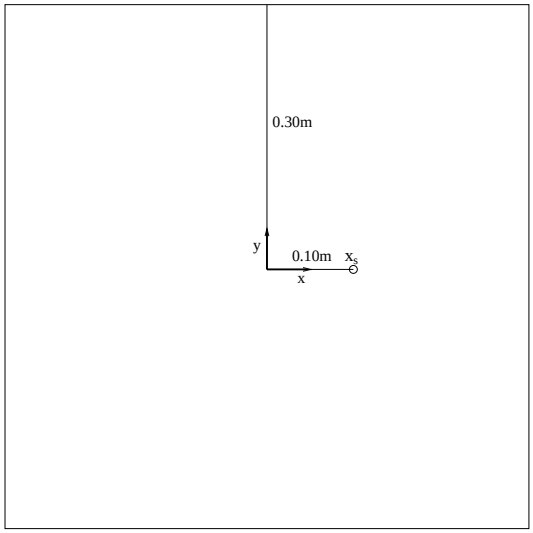

(a)

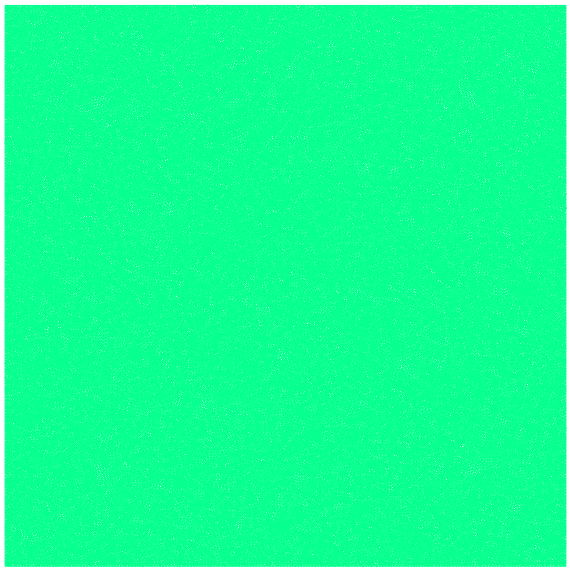

(b)

Fig. 8. (a) Square domain and (b) its mesh.

fully meshed (see Fig.8(b)) and the absorbing condition is put on the exterior boundary. A unit point source is located at point $(0.1m, 0)$ such that the analytical solution is still given by formula (24). The computation is done for $N = 1$ and $N_i = 20$. The mesh is made of 52567 nodes and 104456 elements. Table 6 presents the error on the boundary versus the frequency. It can still

Frequency	DLAC1
10 Hz	0.006
50 Hz	0.005
100 Hz	0.005
500 Hz	0.008
1000 Hz	0.012
2000 Hz	0.017

Table 6
Error e_b on the boundary of the square for different frequencies

be seen that the proposed method leads to low errors at low and medium frequencies. The precedent Bayliss and Turkel method or Feng method would nor be efficient on this type of boundary with straight lines. Figure 9 shows the comparison between the numerical and analytical solutions for the frequencies 50 Hz and 1000Hz. In both cases one can see that the numerical solution is very close to the analytical one

4 Conclusion

A new numerical method has been presented for computing absorbing boundary conditions for the Helmholtz equation. It builds a discrete absorbing matrix directly from the finite element discretisation of the problem. This can be applied to any shape and does not require additional variables or additional domains. So the number of degrees of freedom is the same as for the problem without absorbing boundary conditions. Examples show the accuracy of the method. So, among the methods which do not increase the number of degrees of freedom, this method can be more efficient than those presently used and is rather simple to implement. It is more accurate than these methods and much faster than global methods like the DtN. Similar approaches could be used for other wave propagation problems such as for the propagation of elastic waves.

References

[1] J.B. Keller and D. Givoli. Exact non-reflecting boundary conditions. *Journal of computational physics*, 82(1):172–192, 1989.

[2] D. Givoli and J.B. Keller. A finite element method for large domains. *Computer Methods in Applied Mechanics and Engineering*, 76(1):41–66, 1989.

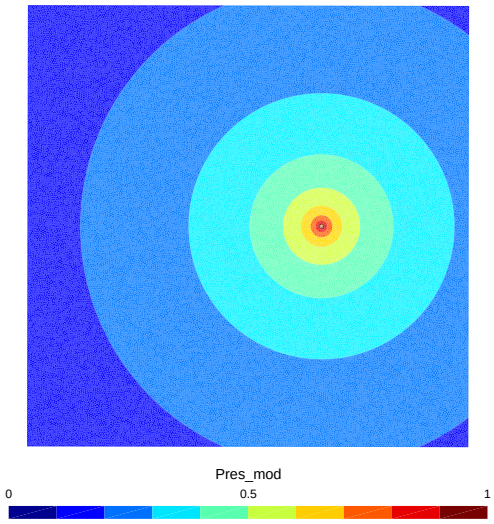

(a) Analytical solution 50 Hz

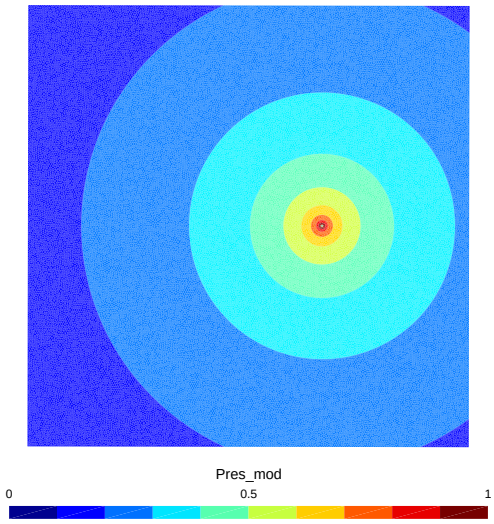

(b) Numerical solution 50 Hz

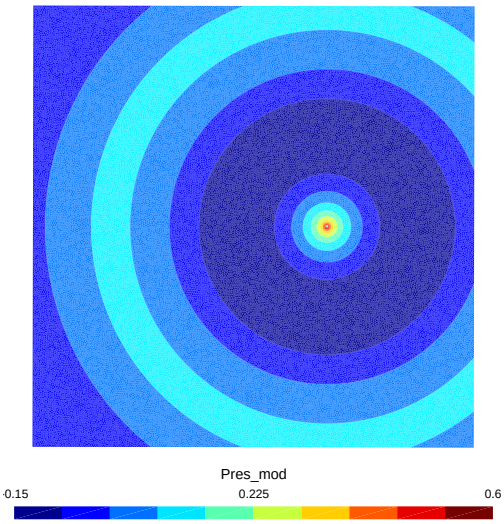

(c) Analytical solution 1000 Hz

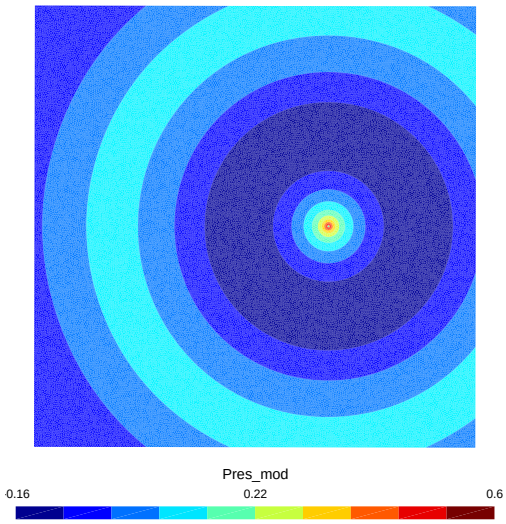

(d) Analytical solution 1000 Hz

Fig. 9. Solutions for a square at 50Hz and 1000Hz

[3] C.A. Brebbia and S. Walker. *Boundary Element Techniques in Engineering*. Newnes-Butterworths, 1980.

[4] R.D. Ciskowski and C.A. Brebbia. *Boundary element methods in acoustics*. Computational mechanics publications, Elsevier Applied Sciences, 1991.

[5] G. Chen and J. Zhou. *Boundary element methods*. Computational mathematics and applications, Academic press, London, England, 1992.

[6] M. Bonnet. *Boundary Integral Equation Methods for Solids and Fluids*. John Wiley and Sons, 1995.

[7] P. Bettess. Infinite elements. *International Journal for Numerical Methods in*

Engineering, 11(1):53–64, 1977.

[8] P. Bettess. More on infinite elements. *International Journal for Numerical Methods in Engineering*, 15(11):1613–1626, 1980.

[9] P. Bettess. *Infinite Elements*. Penshaw Press, 1992.

[10] D.S. Burnett. A three-dimensional acoustic infinite element based on a prolate spheroidal multipole expansion. *Journal of the Acoustical Society of America*, 96:2798–2816, 1994.

[11] R.J. Astley. Infinite elements for wave problems: a review of current formulations and an assessment of accuracy. *International Journal for Numerical Methods in Engineering*, 49(7):951–976, 2000.

[12] K. Gerdes. A review of infinite element methods for exterior helmholtz problems. *Journal of Computational Acoustics*, 8(01):43–62, 2000.

[13] B. Engquist and A. Majda. Absorbing boundary conditions for numerical simulation of waves. *Proceedings of the National Academy of Sciences*, 74(5):1765–1766, 1977.

[14] B. Engquist and A. Majda. Absorbing boundary conditions for numerical simulation of waves. *Mathematics of Computation*, 31(139):629–651, 1977.

[15] R. Clayton and B. Engquist. Absorbing boundary conditions for acoustic and elastic wave equations. *Bulletin of the Seismological Society of America*, 67(6):1529–1540, 1977.

[16] A. C. Reynolds. Boundary conditions for the numerical solution of wave propagation problems. *Geophysics*, 43(6):1099–1110, 1978.

[17] A. Bayliss and E. Turkel. Radiation boundary conditions for wave-like equations. *Communications on Pure and Applied Mathematics*, 33(6):707–725, 1980.

[18] A. Bayliss, M. Gunzburger, and E. Turkel. Boundary conditions for the numerical solution of elliptic equations in exterior regions. *SIAM Journal on Applied Mathematics*, 42(2):430–451, 1982.

[19] J.J. Shirron and I. Babuka. A comparison of approximate boundary conditions and infinite element methods for exterior helmholtz problems. *Computer Methods in Applied Mechanics and Engineering*, 164(1):121–139, 1998.

[20] R.L. Higdon. Absorbing boundary conditions for difference approximations to the multidimensional wave equation. *Mathematics of Computation*, 47(176):437–459, 1986.

[21] R.L. Higdon. Numerical absorbing boundary conditions for the wave equation. *Mathematics of Computation*, 49(179):65–90, 1987.

[22] B. Engquist and A. Majda. Radiation boundary conditions for acoustic and elastic wave calculations. *Communications on Pure and Applied Mathematics*, 32(3):313–357, 1979.

[23] F. Collino. High-order absorbing boundary conditions for wave propagation models. straight line boundary and corner cases. In *Proc. 2nd Int. Conf. on Mathematical & Numerical Aspects of Wave Propagation, R. Kleinmanet al.SIAM*, pages 161–171, Delaware, USA, 1993.

[24] T. Hagstrom and S.I. Hariharan. A formulation of asymptotic and exact boundary conditions using local operators. *Applied Numerical Mathematics*, 27(4):403 – 416, 1998.

[25] J.H. Lee and J.L. Tassoulas. Absorbing boundary condition for scalar-wave propagation problems in infinite media based on a root-finding algorithm. *Computer Methods in Applied Mechanics and Engineering*, 330:207–219, 2018.

[26] D. Givoli. High-order local non-reflecting boundary conditions: a review. *Wave Motion*, 39(4):319–326, 2004.

[27] C. Cerjan, D. Kosloff, R. Kosloff, and M. Reshef. A nonreflecting boundary condition for discrete acoustic and elastic wave equations. *Geophysics*, 50(4):705–708, 1985.

[28] J. Sochacki, R. Kubichek, J. George, W. R. Fletcher, and S. Smithson. Absorbing boundary conditions and surface waves. *Geophysics*, 52(1):60–71, 1987.

[29] J.P. Berenger. A perfectly matched layer for the absorption of electromagnetic waves. *Journal of computational physics*, 114(2):185–200, 1994.

[30] J.P. Berenger. Three-dimensional perfectly matched layer for the absorption of electromagnetic waves. *Journal of computational physics*, 127(2):363–379, 1996.

[31] F. Collino and P.B. Monk. Optimizing the perfectly matched layer. *Computer methods in applied mechanics and engineering*, 164(1):157–171, 1998.

[32] S. Asvadurov, V. Druskin, M.N. Guddati, and L. Knizhnerman. On optimal finite-difference approximation of PML. *SIAM Journal on Numerical Analysis*, 41(1):287–305, 2003.

[33] D. Givoli. Non-reflecting boundary conditions. *Journal of Computational Physics*, 94(1):1–29, 1991.

[34] D. Rabinovich, D. Givoli, and E. Bécache. Comparison of high-order absorbing boundary conditions and perfectly matched layers in the frequency domain. *International Journal for Numerical Methods in Biomedical Engineering*, 26:1351–1369, 2010.

[35] Y. Gao, H. Song, J. Zhang, and Z. Yao. Comparison of artificial absorbing boundaries for acoustic wave equation modelling. *Exploration Geophysics*, 48(1):76–93, 2017.

[36] D. Duhamel and T.M. Nguyen. Finite element computation of absorbing boundary conditions for time-harmonic wave problems. *Computer Methods in Applied Mechanics and Engineering*, 198(37):3006–3019, 2009.

[37] S. Thirunavukkarasu and M.N. Guddati. Absorbing boundary conditions for time harmonic wave propagation in discretized domains. *Computer Methods in Applied Mechanics and Engineering*, 200(33):2483 – 2497, 2011.

[38] D. Givoli, I. Patlashenko, and J.B. Keller. Discrete Dirichlet-to-Neumann maps for unbounded domains. *Computer Methods in Applied Mechanics and Engineering*, 164:173–185, 1998.

[39] D. Colton. Runges theorem and far field patterns for the impedance boundary value problem in acoustic wave propagation. *SIAM Journal on Mathematical Analysis*, 13(6):970–977, 1982.

[40] R.F. Millar. On the completeness of sets of solutions to the helmholtz equation. *IMA Journal of Applied Mathematics*, 30(1):27–37, 1983.

[41] Y. Liu and J.S. Bolton. On the completeness and the linear dependence of the cartesian multipole series in representing the solution to the helmholtz equation. *The Journal of the Acoustical Society of America*, 140(2):EL149–EL153, 2016.

[42] H. Gan, P.L. Levin, and R. Ludwig. Finite element formulation of acoustic scattering phenomena with absorbing boundary condition in the frequency domain. *The Journal of the Acoustical Society of America*, 94(3):1651–1662, 1993.

[43] K. Feng. Finite element method and natural boundary reduction. In *Proc. of the International Congress of Mathematicians*, pages 1439–1453, Warszawa, Poland, 1983.